Crosstalk Detection in Signalized-Intersection Loop Detectors

Joseph M. Ernst, Dhruv Lamba, James V. Krogmeier, and Darcy M. Bullock

Electromagnetic sensors, such as inductive loops and microloops, are widely used for vehicle detection. However, electrical coupling can occur between detection devices and result in electrical noise called crosstalk, which significantly degrades detection operation. Techniques such as channel scanning and frequency separation have been used to mitigate crosstalk; however, crosstalk is often transient because of environmental conditions and not always observed easily. This paper presents a crosstalk detection algorithm based on 156 h of training data taken from 12 sensors (inductive and microloop) and applies it to approximately 14 h of data collected from seven sensors (four inductive loops and three microloops) to demonstrate an automated method to identify periods when crosstalk occurs. The paper concludes by recommending the use of this approach for system acceptance and ongoing monitoring of sensor health.

Electromagnetic sensors, particularly inductive loops and microloops, have been used for vehicle detection since the late 1960s (*1*). Although robust, these devices are susceptible to crosstalk due to interference from adjacent electrical devices. Crosstalk may lead to false detections and cause severe problems in detector operation (*2–4*). Several authors have described crosstalk in electromagnetic detection systems as a challenge to be addressed (*2–7*). Crosstalk noise can cause false detections, degrade vehicle count information, cause errors in estimation of demand at intersections, and cause poor segmentation for vehicle matching and speed estimation algorithms.

Inductive loops and microloops are sensors whose inductance varies in response to a vehicle. The change in inductance is manifested as a frequency change in a tuned circuit and is measured by a detector card. The detector cards used in this study measure this change in frequency by comparison with a standard 32-MHz crystal oscillator and were provided by Eberle Design Inc. (EDI) and 3M. The difference in the period of the loop oscillator waveform and the period of a reference waveform (corresponding to no vehicle present) is reported as a number of "counts" of the standard 32-MHz oscillator. A time-varying series of these measurements in counts is called a "signature" in this paper.

Crosstalk is typically caused by inductive or capacitive coupling between closely placed loops or closely spaced lead in wires operating at similar frequencies (*2*). Poor-quality connections and wires sharing a common conduit are two of the factors that aggravate this coupling (*2*).

School of Civil Engineering, Purdue University, 550 Stadium Mall Drive, West Lafayette, IN 47906. Corresponding author: D. M. Bullock, darcy@purdue.edu.

Transportation Research Record: Journal of the Transportation Research Board, No. 2192, Transportation Research Board of the National Academies, Washington, D.C., 2010, pp. 50–63.
DOI: 10.3141/2192-05

Crosstalk elimination is difficult because crosstalk may exist in multiple frequency bands, which may change over time due to environmental factors. Efforts to remove crosstalk (using filtration techniques) were reported as early as 1986 (*8*). Today, the *Traffic Detector Handbook* gives detailed instructions for avoiding and removing crosstalk (*2*); however, the transient nature of crosstalk makes it hard to know when to apply the mitigating measures.

A crosstalk detection algorithm is needed, because, unlike a crosstalk removal tool, it does not mask the underlying problems, such as improper cable shield connections or channels that have drifted into overlapping bands due to environmental factors, that may be causing crosstalk (*2*). A crosstalk detection algorithm indicates the possibility of these problems at the installation. It is more beneficial to fix the causes of crosstalk than to filter the symptoms (i.e., noisy signatures).

Although physical characteristics (e.g., loop spacing, frequency separation) causing crosstalk have been studied (*3*) and macroscopic speed estimate discrepancies have been used as an indication of crosstalk (*6*), these methods do not measure crosstalk in the signal itself. This paper improves crosstalk detection by developing a signal-processing algorithm on the basis of loop signal data itself, to identify objectively (and quantify) the presence of crosstalk in a system.

OBJECTIVES

This paper first defines details about the test data collected. The detection algorithm section then explains the crosstalk detection algorithm proposed. The algorithm is applied to the data collected, and the outcomes are summarized in the results section. Based on the results, recommendations are made for future work in the section on future applications. The validity and implications of the algorithm are finally discussed in the section that covers conclusions, where recommendations are made for the implementation of frequency analysis of loop sensor data to measure quantitatively the amount of crosstalk present.

DATA COLLECTION

The algorithm was designed by using 156 h of development data collected from 12 sensors, including both inductive loops and microloops (a type of magnetometer). In addition, seven sets of evaluation data were collected on 2 days. Test IDs 1 through 4 were simultaneously collected on March 23, 2007, for 2 h 35 min each, by means of inductive loop sensors. Test IDs 5 through 7 were simultaneously collected on May 15, 2009, for 57 min each, by means of microloop sensors. All these sensors were within 150 ft of the stop bar (or closer) and subject to extended presence due to vehicle queuing. Details for the seven testing data sets are summarized in Table 1. The noise in Test IDs 5

TABLE 1 Example Sensor Performance Table Summarizing Amount of Crosstalk Present in Data Collected

Test ID	Sensor Name	Date	Duration of Waveform (s)	Duration of Crosstalk (s)	Percentage of Signal Containing Crosstalk
1	NA_L6	03/23/2007	9,277	1,503	16.2
2	NA_L8	03/23/2007	9,277	1,112	12.0
3	NB_L6	03/23/2007	9,264	881	9.5
4	NB_L8	03/23/2007	9,264	901	9.7
5	NA_M1	05/15/2009	3,451	0	0
6	NA_M7	05/15/2009	3,451	2,393	69.3
7	NB_M7	05/15/2009	3,451	2,327	67.4

to 7 can be eliminated by adjusting the frequency settings of the detector cards. This implies that the noise is due to crosstalk between the sensors. In addition, Test IDs 1 to 4 have a periodic nature that is indicative of crosstalk. For these reasons, the authors believe that the noise being detected is in fact crosstalk.

CROSSTALK DETECTION ALGORITHM

This section develops a crosstalk detection algorithm. The first subsection begins by describing the qualitative features of data with and without crosstalk. The data are then analyzed in the frequency domain by using the Fourier transform. An algorithm for measuring the spectral energy due to crosstalk is subsequently proposed. Finally, the algorithm is trained to differentiate between data with and without crosstalk.

Characterization of Signatures with Crosstalk in Time Domain

The time-varying waveform corresponding to the change in oscillating frequency of the sensor circuit due to a passing vehicle is termed a "signature."

Ideally, the detector's oscillation frequency is influenced only by the presence of a vehicle over the sensor. But, in some situations, the signals of independent detector circuits may be coupled to each other and causes a spurious change in the oscillation frequency, which here is being called crosstalk. This is illustrated in Figure 1, which shows a 2.5-h signature train containing varying levels of crosstalk. Figures 1*a*, 1*b,* and 1*c* show three 10-s segments extracted from the longer train of Figure 1*d.* In Figure 1*a*, no crosstalk is evident while Figures 1*b* and 1*c* show increasing levels of crosstalk interference. The crosstalk in this example manifests itself as random noise added to the vehicle-induced signatures.

Figure 2 shows another form of crosstalk, which is manifested as sinusoidal harmonics in the signal. This is similar to the beating effect of two frequencies observed from two instruments at extremely close frequencies (or pitches). Both the more-random and beating types of crosstalk include high-frequency noise. This noise can be separated from the signature influenced by the vehicles because the effect of vehicles on the sensor is limited by their speed and the size of their metallic components that affect the sensor. These factors generate waveforms that tend to stay below 10 Hz. Therefore, the energy in the signatures at frequencies more than 10 Hz must be primarily due to crosstalk interference.

Characterization of Signatures with Crosstalk in Frequency Domain

Because crosstalk and vehicular signatures can be separated in frequency, a frequency domain analysis is useful. The fast Fourier transform (FFT) is used to determine the contribution of each frequency to the signal. The frequency domain representation of each 1,000-sample block of the signal is then generated. This corresponds to approximately 10 s of data. The magnitude of the frequency content of the signal can then be analyzed. Figures 3*a* through 3*d* are four 10-s signatures, and Figures 3*e* through 3*h* are their respective frequency domain representations as calculated by FFT.

The top pair of plots shows that, if there is no vehicle and no crosstalk, there is nothing in the time domain or frequency domain. The second pair shows the time and frequency domain plots of a signature that is only affected by a vehicle. As discussed in the preceding section, the frequency of the vehicle is limited to about 10 Hz. The purely crosstalk signature and frequency representation in the third row show that the crosstalk-influenced signature has frequency components in all possible frequencies. Because the time domain signature is sampled, the possible frequencies are from 0 Hz to half the sampling frequency. The last signature has crosstalk effects and is also affected by a passing vehicle. The effects are superimposed in the time and frequency domain such that the fourth pair resembles the second and third pair added together. The following discussion develops an algorithm to detect crosstalk.

Spectral Energy Analysis

From the observations in the first two subsections, a metric to characterize the amount of crosstalk is now proposed. First, the signature is broken into vectors of length N, where $N = 1{,}000$ samples. Each vector $\bar{x}[n]$ is then processed by an algorithm depicted in the block diagram in Figure 4*a.* The algorithm begins by multiplying $\bar{x}[n]$ with a 1,000-point Gaussian window $\bar{w}_G[n]$. The Gaussian window is chosen as it has the minimum time–bandwidth product among all tapered windows, allowing for maximum resolution in the frequency domain. A rectangular window was not chosen because of its high side lobes in the frequency domain, which reduce spectral resolution.

The resulting windowed data vector $\bar{s}[n]$ is then considered in the frequency domain using an FFT to yield the frequency domain signal $\bar{S}[k]$.

From the frequencies of signatures shown in Figures 3*e* and 3*f*, it may be deduced that detections usually lie in the 0- to 10-Hz range while crosstalk affects the band outside this range. Hence, the out-of-band

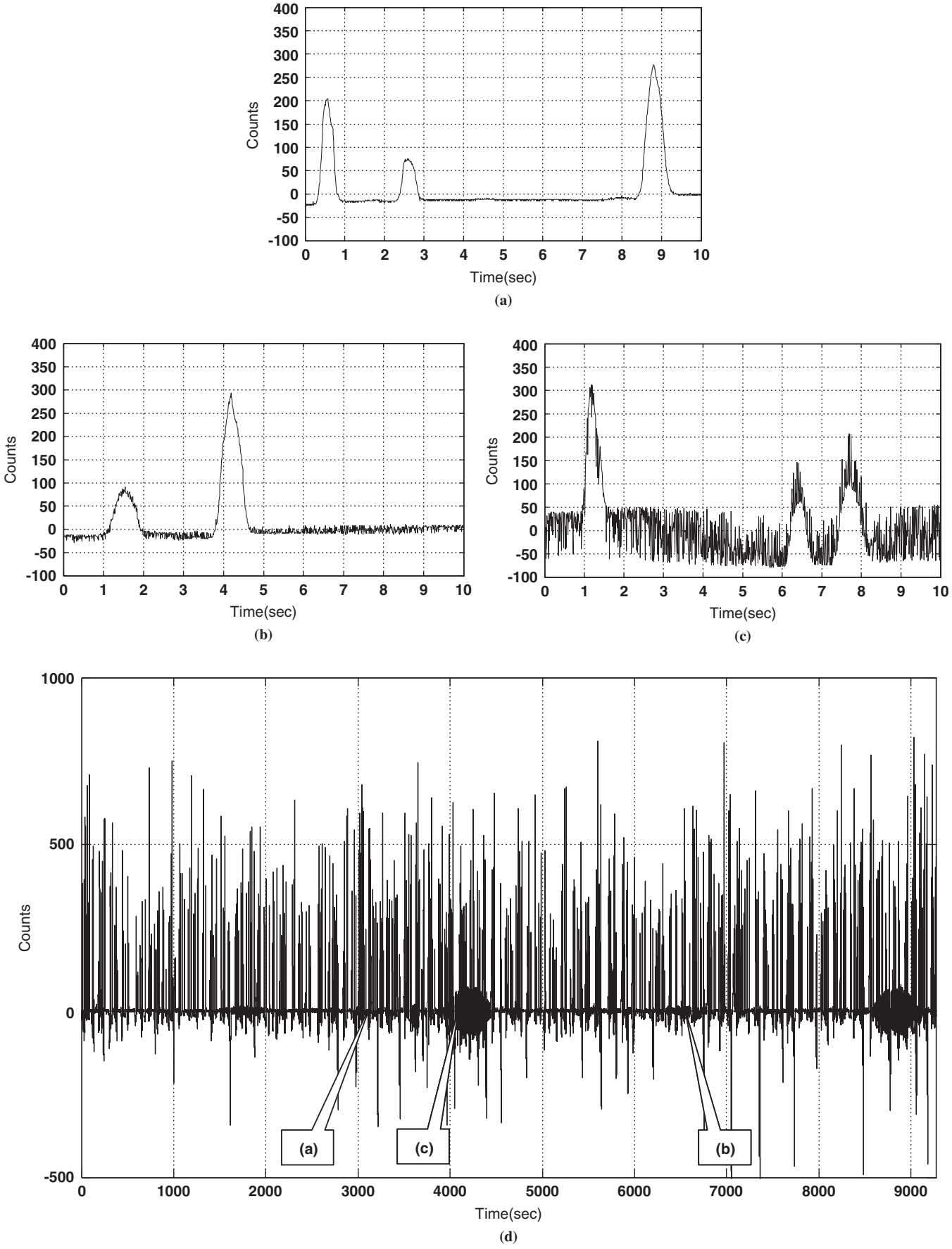

FIGURE 1 Example signatures showing varying levels of effect of crosstalk (Test ID 1): (*a*) 10-s signature starting at t_1 = 3,170 s, with no crosstalk; (*b*) 10-s signature starting at t_2 = 6,517 s, with slight crosstalk; (*c*) 10-s signature starting at t_3 = 4,150 s, with significant crosstalk; and (*d*) 2.5-h waveform.

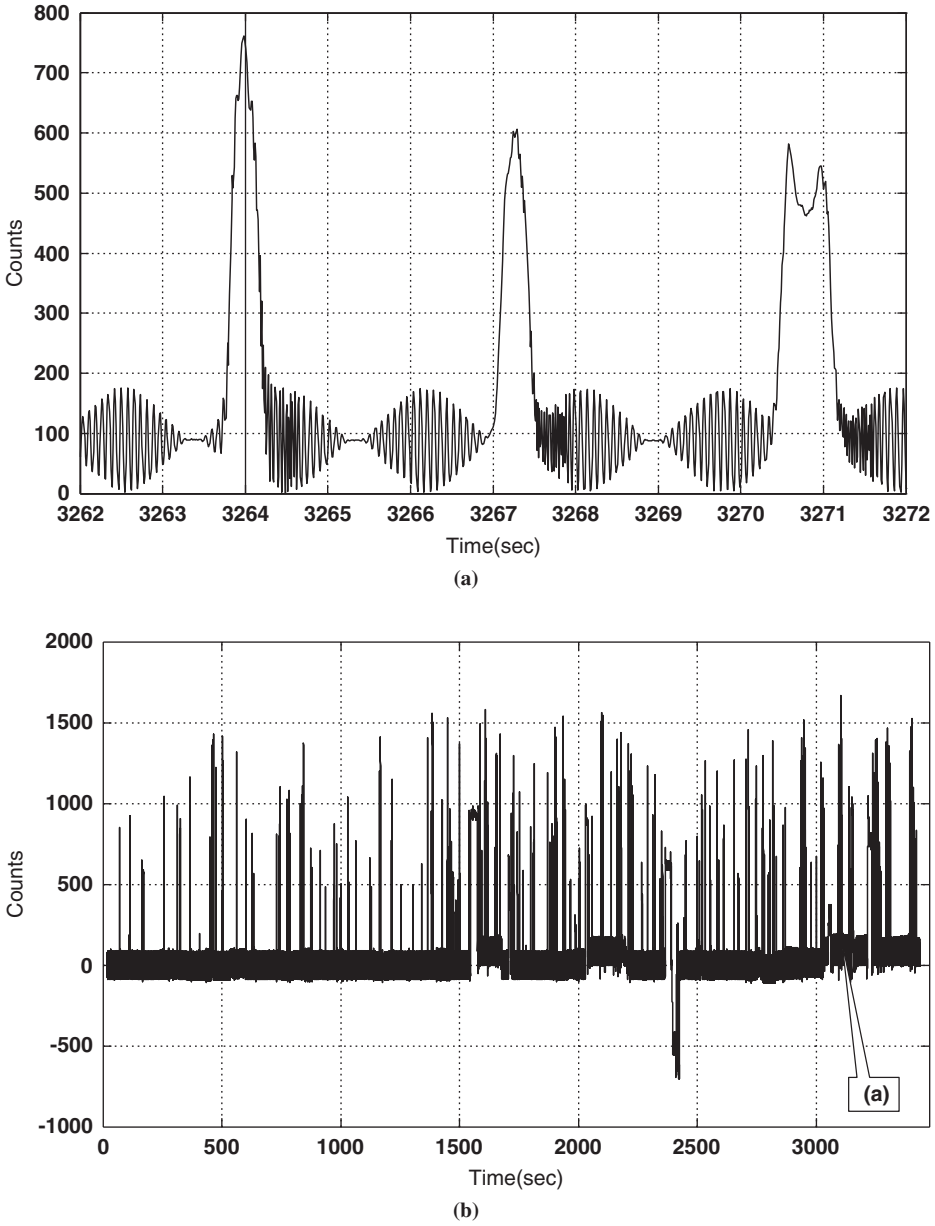

FIGURE 2 Signature showing harmonic crosstalk beats (Test ID 7): (*a*) 10-s signature starting at t = 3,262 s, with substantial amount of crosstalk-caused beats, and (*b*) 57-min waveform.

spectral energy is used as a measure for the amount of crosstalk. The 0- to 10-Hz frequency range corresponds to the discrete range

$$k \in \left(\frac{10N}{F_s}, \text{floor}\left(\frac{N}{2} \right) \right) \tag{1}$$

where

k = FFT index,
F_s ($= n_{\text{total}}/T$) = sampling rate,
n_{total} = total number of samples in data set, and
T = total duration of data set.

The out-of-band energy for $\bar{x}[n]$ is labeled $\bar{E}_{\text{out}}$ in Figure 4*a* and is found by summing the magnitude of $\bar{S}[k]$ over the range shown in Equation 1. $\bar{E}_{\text{total}}$ is then found as the total spectral energy from positive frequencies in $\bar{S}[k]$, corresponding to the discrete range

$$k \in \left(0, \text{floor}\left(\frac{N}{2} \right) \right) \tag{2}$$

$\bar{E}_{\text{out}}$ is then divided by the maximum of $\bar{E}_{\text{total}}$ over the previous M vectors, where M is large enough that $\bar{E}_{\text{total}}$ includes a window with a vehicle and thus characterizes the total possible spectral energy in a signature. This number M can be set on the basis of traffic conditions. The ratio $E_{\text{out}}/\max\{E_{\text{total:past}}\}$ is expressed as a percentage to make the crosstalk index less dependent upon the installation.

This percentage is labeled $\bar{T}(x)$ in Figure 4*a* and referred to as the crosstalk index throughout this paper. The evaluation of

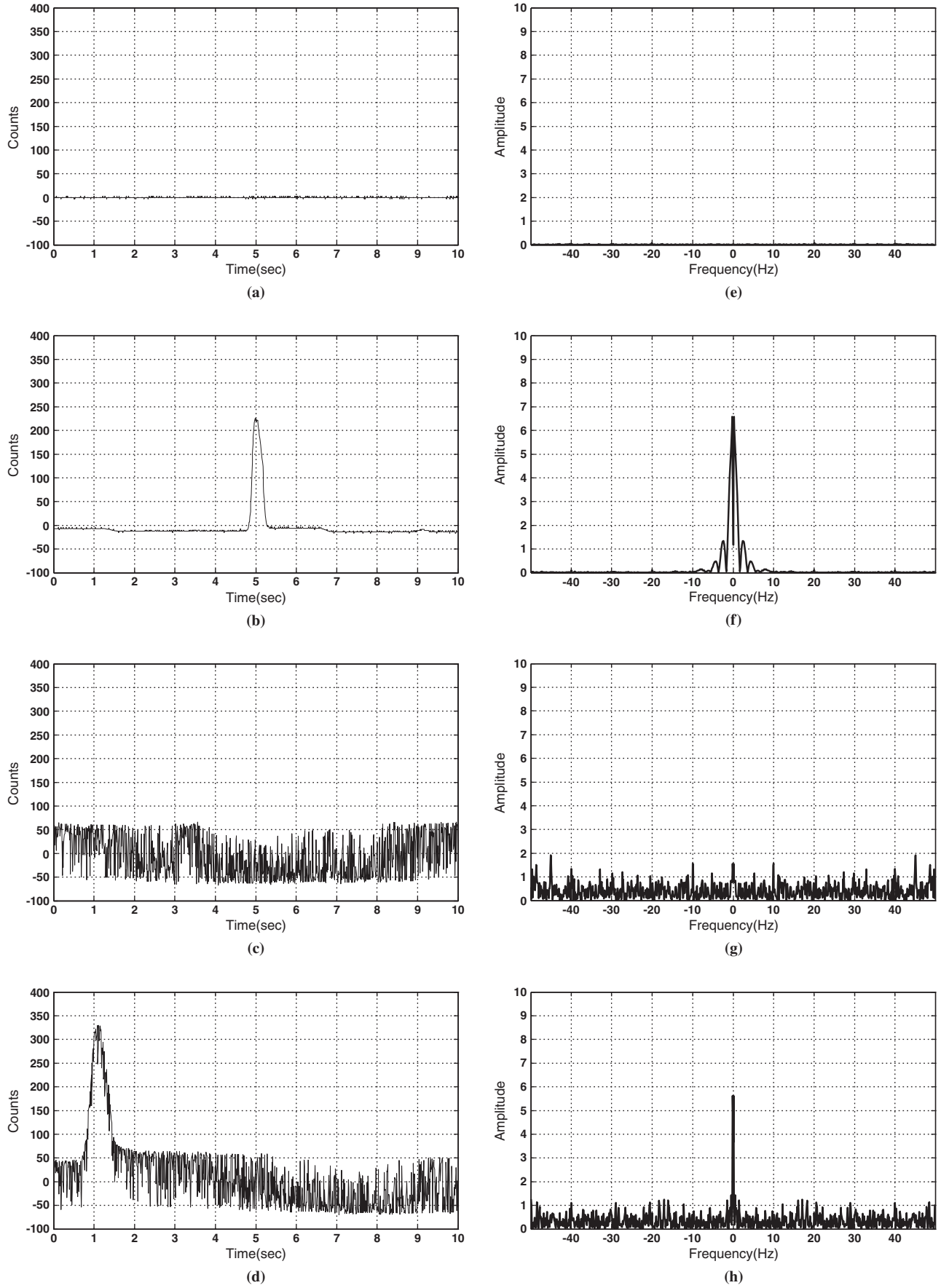

FIGURE 3 Short duration (10-s) data sets illustrating difference in spectral content between regions with and without crosstalk (Test ID 1): (a) signature with no detections and no crosstalk, (*b*) signature with single detection and no crosstalk, (*c*) signature with crosstalk but no detections, (*d*) signature with single detection and crosstalk, (*e*) FFT of signature with no detections and no crosstalk, (*f*) FFT of signature with single detection and no crosstalk, (*g*) FFT of signature with crosstalk but no detections, and (*h*) FFT of signature with single detection and crosstalk.

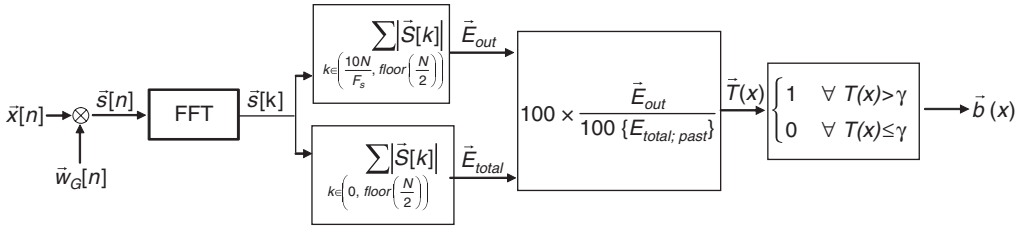

(b)

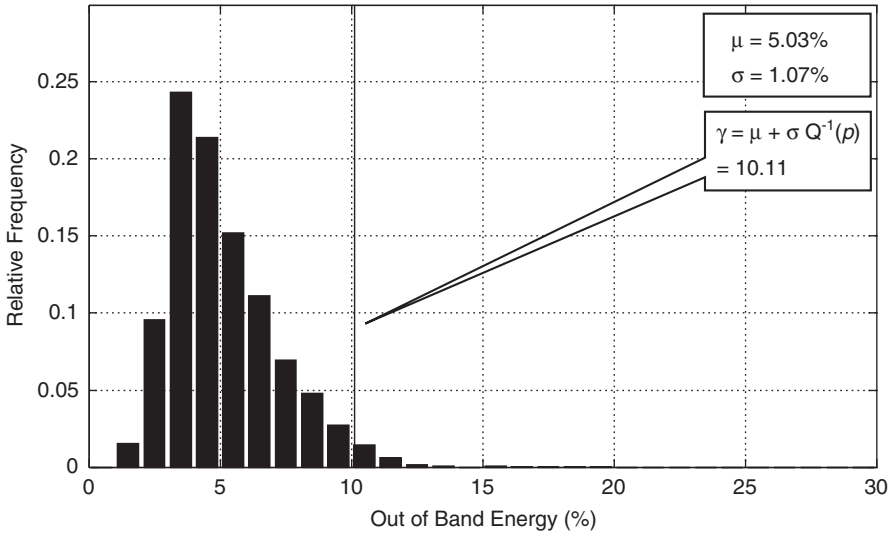

(b)

FIGURE 4 Development of metric threshold that uses test statistic developed by frequency analysis: (*a*) block diagram of algorithm to provide a metric for out-of-band energy to identify crosstalk and (*b*) histogram of crosstalk index for 108 sample waveforms (156 h total) to estimate threshold for detecting crosstalk.

threshold γ and the binary crosstalk indicator $\bar{b}(x)$ is presented in the next subsection.

Determination of Crosstalk Index Threshold

This crosstalk index is evaluated for 156 h of data collected from 12 sensors at an installation that has shown no signs of crosstalk. A histogram of the points for these crosstalk indices is shown in Figure 4*b*. This is a statistically significant data set with which to characterize the algorithm's performance over data with no crosstalk. In the Neyman–Pearson framework, this is the null hypothesis. Even though the distribution does not appear to be Gaussian, a Gaussian distribution is assumed to characterize this crosstalk index.

Neyman–Pearson is a theory framework from statistics. The property being used for this analysis is that the false alarm rate can be chosen through the threshold with knowledge only of the null hypothesis.

The distribution is found to have a mean of $\mu = 5.03$ and a variance of $\sigma = 1.07$. With these values and the Gaussian assumption, a threshold can be set by limiting the probability of Type I error (e.g., detecting crosstalk when it is not present) to .001%. The threshold is found by applying the following formula:

$$\gamma = \mu + \sigma Q^{-1}(p) \tag{3}$$

where p is the probability of Type 1 error as defined above and $Q(x)$ is the complementary cumulative distribution functions (CDFs) of a Gaussian random variable (*9*). A threshold of $\gamma = 10.11\%$ is thus obtained and is shown as the solid vertical line in Figure 4*b*. This means that any crosstalk index above 10.11% will be flagged as an indication of crosstalk.

Finally, the crosstalk index is passed through a threshold function that is based on the estimated threshold γ, which produces a binary crosstalk indicator $\bar{b}(x)$. The binary indicator turns on when the crosstalk index $\bar{T}(x)$ crosses the calculated threshold $\gamma = 10.11\%$ and stays off otherwise. This indicates that crosstalk is present when $\bar{T}(x)$ is larger than γ and absent otherwise.

RESULTS FROM CROSSTALK DETECTION ALGORITHM

The results section shows that the crosstalk detection algorithm accurately detects both the random noise and ringing types of crosstalk by analyzing 14 h of data from seven sensors (four inductive loops and three microloops). It also shows that this algorithm can be used to characterize the severity of the crosstalk if it exists.

Figure 5 shows the application of the algorithm to data set Test ID 1, which exhibits the random noise type of crosstalk that tends to come and go over long periods. As expected, the crosstalk index $\bar{T}(x)$

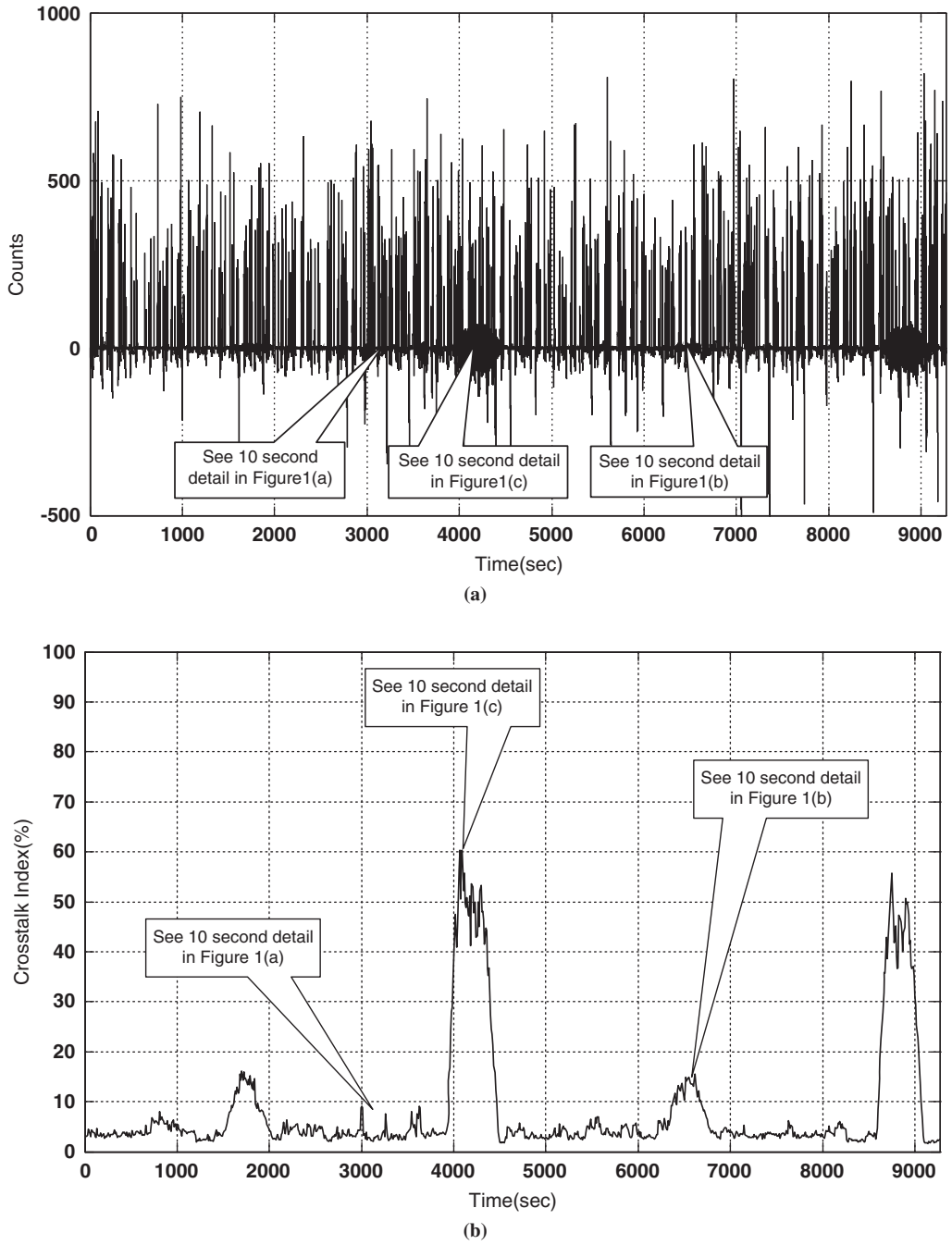

FIGURE 5 Illustration of significant increase in out-of-band energy during periods of crosstalk (Test ID 1): (*a*) example 2.5-h waveform and (*b*) crosstalk index $\bar{T}(x)$.

can be seen to increase significantly in regions where severe crosstalk exists (e.g., around both 4,000 and 8,500 s). It also shows affected areas around 2,000 and 6,500 s that are not readily apparent on a macroscopic view of the data but were verified to have crosstalk, as previously shown in Figure 1*b*.

Figure 6 shows the application of the algorithm to data sets Test IDs 2 and 3. The crosstalk detection algorithm performed similarly on these data sets as on Test ID 1. One unexpected spike occurred in the crosstalk index at approximately 2,404 s in Figure 6*b*. This can be attributed to a communication error at that time, as the detailed signature shows in Figure 7*a*. The offending signature, labeled (i) in Figure 7*a*, shows the signal dropping in magnitude in an infinitesimally small time, causing a high-frequency component. This frequency lies outside the normal signature frequency band, and its effect is reflected as the spike labeled (ii) in the crosstalk index shown in Figure 7*b*. Test ID 4 also performed similar to Test ID 2 because it is a similar type of crosstalk.

Figure 8 shows the application of the algorithm to data sets Test IDs 5 and 6. Test ID 5 shows an example of a sensor that is unaffected by crosstalk. The crosstalk index remains close to zero throughout

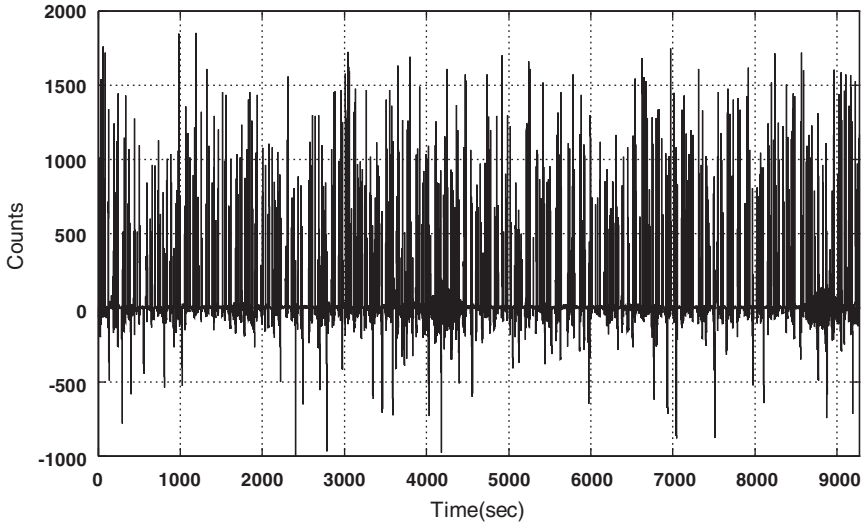

(a)

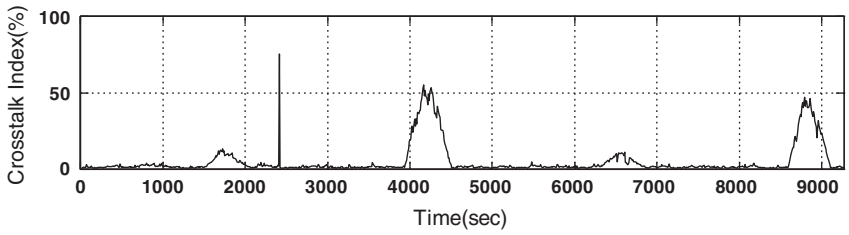

(b)

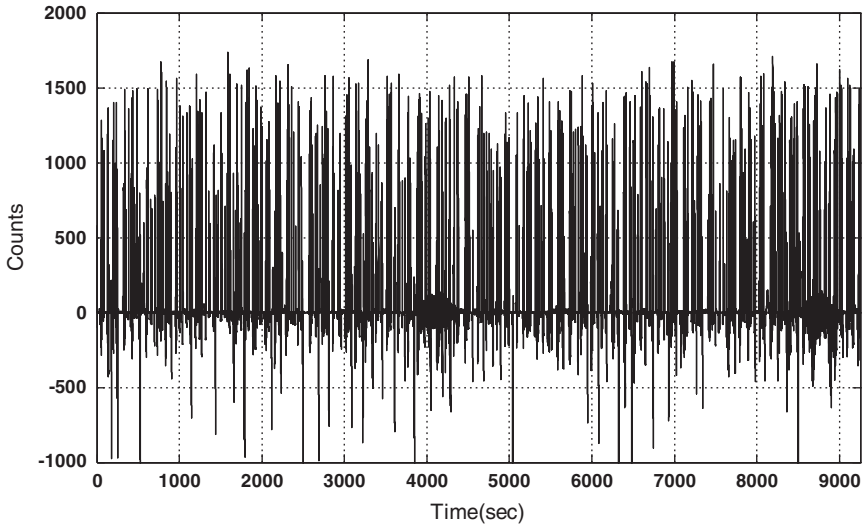

(c)

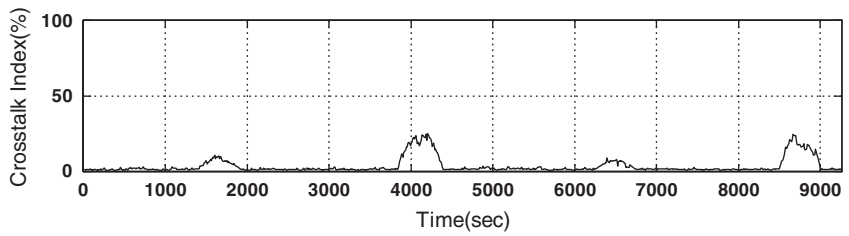

(d)

FIGURE 6 Example crosstalk indices for long-period, short-duration crosstalk in data sets from inductive loop sensors: (*a*) example 2.5-h waveform (Test ID 2), (*b*) crosstalk index (Test ID 2), (*c*) example 2.5-h waveform (Test ID 3), and (*d*) crosstalk index (Test ID 3).

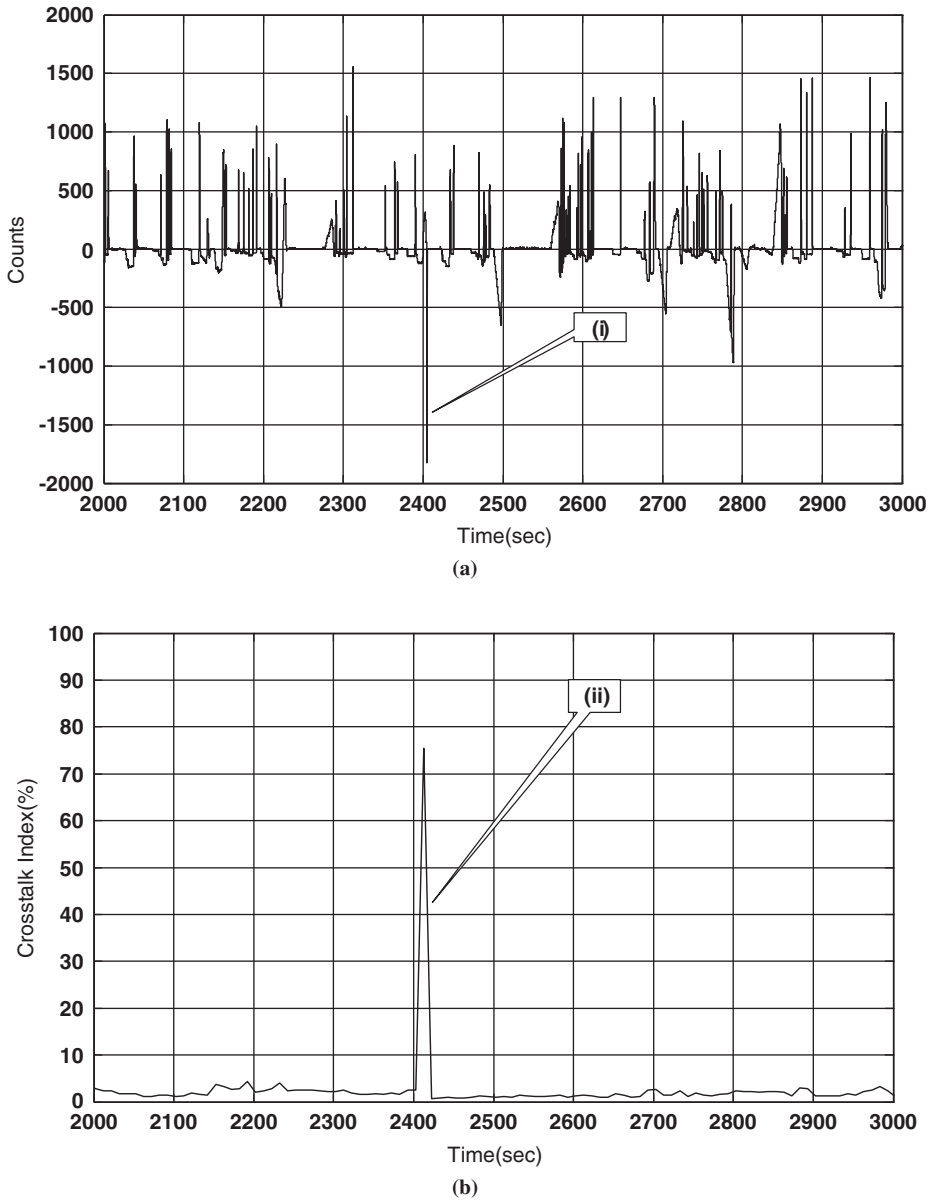

FIGURE 7 Sample signature showing effect of bit errors on crosstalk metric (Test ID 2): (*a*) example 1,000-s signature with communication error at approximately t = 2,404 s and (*b*) crosstalk index plot with communication error at approximately t = 2,404 s.

the entire data set. Test ID 6 shows continuous crosstalk that is clearly seen in the original signal in Figure 8*c* and in the crosstalk index Figure 8*d*.

Figure 9 shows two ways of visualizing the crosstalk in Test ID 1. The binary crosstalk indicator shown in Figure 9*a* clearly shows the times at which crosstalk was present in the signal. Figure 9*b* shows the severity of the crosstalk. A threshold of approximately 10 was chosen in the algorithm development section. When this threshold is used, no crosstalk is present 83.8% of the time and crosstalk is present 16.2% of the time.

Figure 10 shows the crosstalk index, binary crosstalk indicator, and CDFs for Test ID 2, a data set for which crosstalk tends to come and go over time. Test IDs 3 and 4 have similar plots not shown. Test ID 5 represents the data sets with no crosstalk. Test ID 6 represents the data sets with continuously ringing crosstalk. Test ID 7 is similar to Test ID 6 but is not shown. The evidence that this crosstalk detector works is that the intermittent crosstalk shown in Figure 10*a* yields only crosstalk detected 12% of the time in Figure 10*b*. Likewise, there is no crosstalk in Figure 10*c*, and crosstalk is detected 0% of the time. Figure 10*e* shows continuous ringing crosstalk and Figure 10*f* shows a corresponding high percentage of crosstalk of 69.3%.

FUTURE APPLICATIONS

Through Figure 11 comes the suggestion of a possible implementation of the algorithm on portable diagnostic equipment. This equipment could monitor the performance of several sensors and provide a log of crosstalk activity.

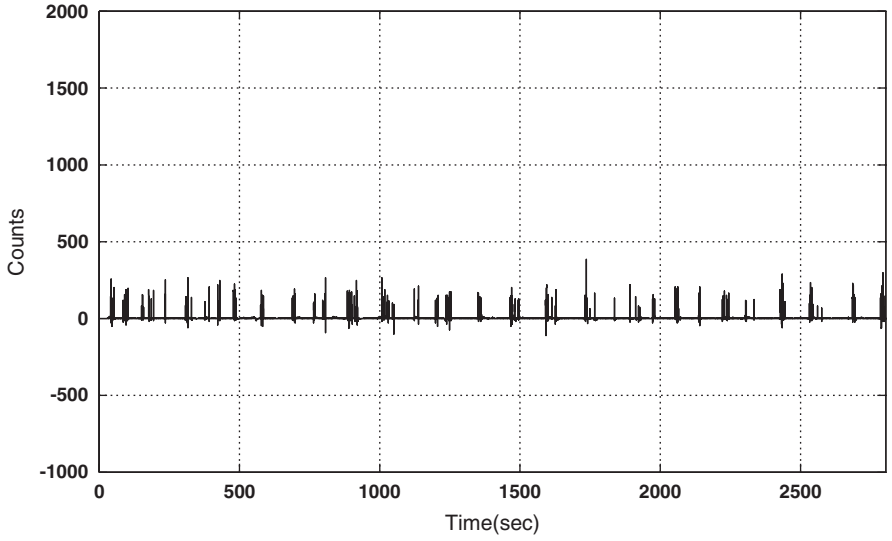

(a)

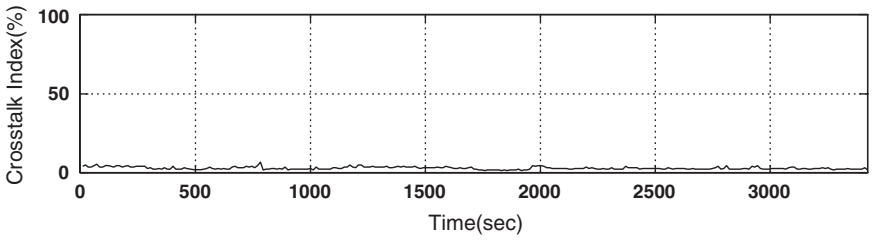

(b)

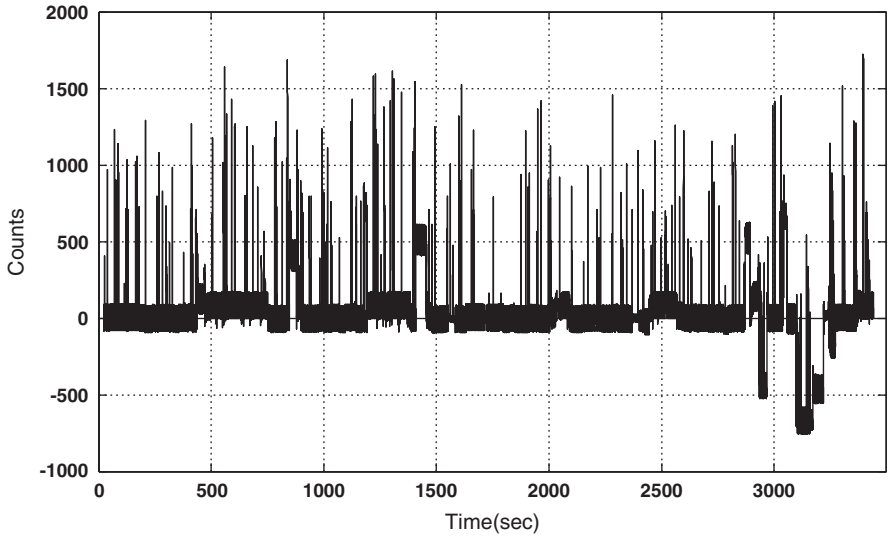

(c)

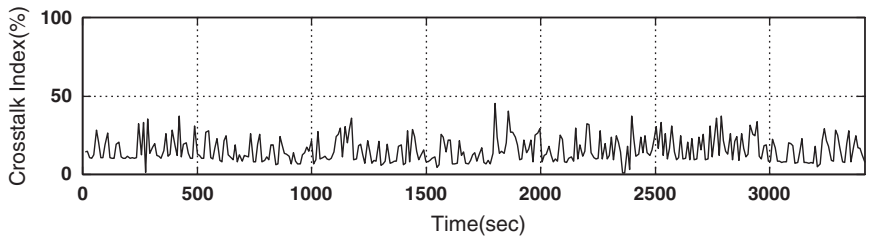

(d)

FIGURE 8 Comparison of crosstalk indices for data set with no crosstalk (Test ID 5) and data set with continuous ringing crosstalk (Test ID 6): (*a*) example 57-min waveform (Test ID 5), (*b*) crosstalk index (Test ID 5), (*c*) example 57-min waveform (Test ID 6), and (*d*) crosstalk index (Test ID 6).

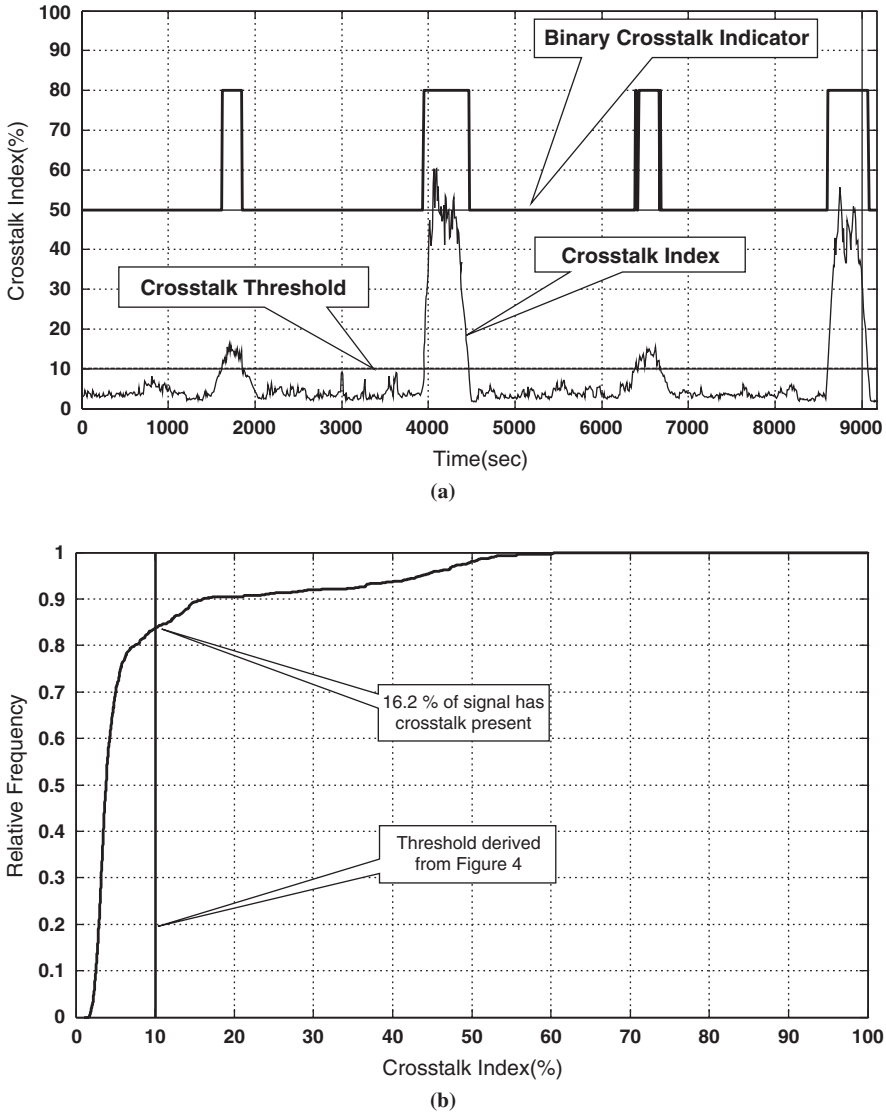

FIGURE 9 CDF for crosstalk index (Test ID 1) showing percentage of data containing crosstalk (with distinct regions of crosstalk): (*a*) crosstalk index and binary metric and (*b*) CDF of crosstalk index.

The hardware would acquire data and run the algorithm continuously. The hardware could be configured to produce a report of the system's health that may be used to assess the performance of the system during an extended period, say 24 h. Table 1 shows a report for a short duration that is based upon the data sets identified in Table 2.

This type of algorithm can be implemented by a simple microcontroller with an inexpensive FFT chip. In the short term, it could be done as an external interface through the data port of the detector card and the same interface used for collecting the data. In the longer term, this type of algorithm could be implemented on the detector card itself, with no external hardware required.

Figure 11 offers a hypothetical report that may be generated by using the crosstalk detection system. Looking at the final column containing statistics of crosstalk, installation staff may easily discern that Channels 4, 6, and 8 have significant amounts of crosstalk and need attention. Longer term, because crosstalk can usually be removed by separating the frequency of channels that have drifted into a common frequency band, the system might ultimately evolve to the point where it could automatically configure the frequency settings of the detector cards.

CONCLUSION

This paper proposes a theoretically sound model that is signal-processing based to quantify the out-of-band energy due to crosstalk in a loop detector signal. Examples of different types and magnitudes of crosstalk are illustrated in Figures 1 and 2. Figure 3 is used to demonstrate that the frequency domain analysis of the signatures vividly illustrates the presence of crosstalk. Figure 4 introduces a model that is signal-processing based to identify a crosstalk index from out-of-band energy observed in the frequency domain analysis.

The application of this crosstalk index to more than 14 h of raw loop detector data is presented in Figures 5 through 8. Figure 9 shows

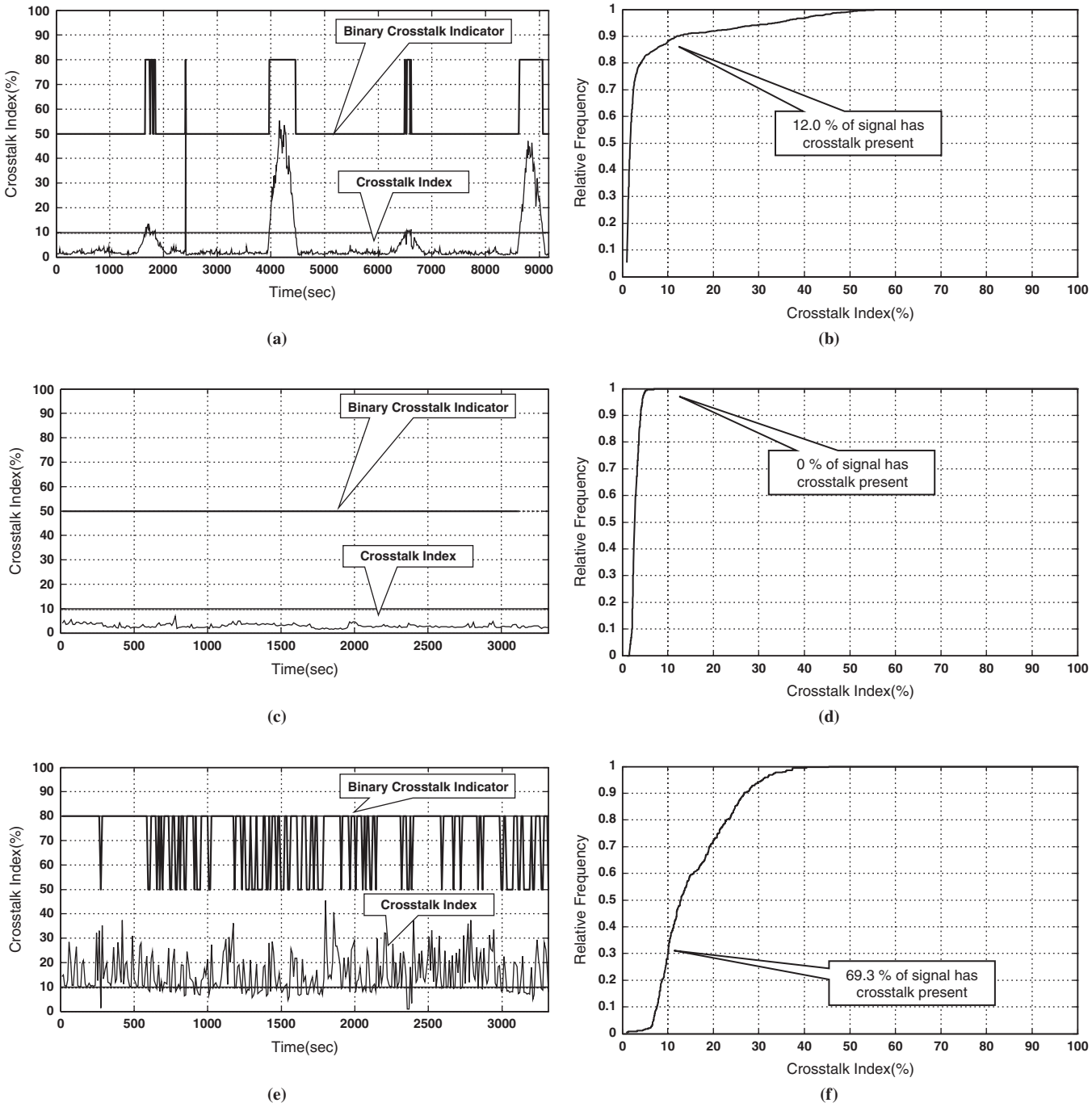

FIGURE 10 Binary crosstalk indicators, crosstalk index, and CDFs for selected data sets: (*a*) crosstalk index and binary crosstalk indicator for Test ID 2 (distinct regions of crosstalk), (*b*) CDF of crosstalk index for Test ID 2 (distinct regions of crosstalk), (*c*) crosstalk index and binary crosstalk indicator for Test ID 5 (no crosstalk), (*d*) CDF of crosstalk index for Test ID 5 (no crosstalk), (*e*) crosstalk index and binary crosstalk indicator for Test ID 6 (continuous crosstalk), and (*f*) CDF of crosstalk index for Test ID 6 (continuous crosstalk).

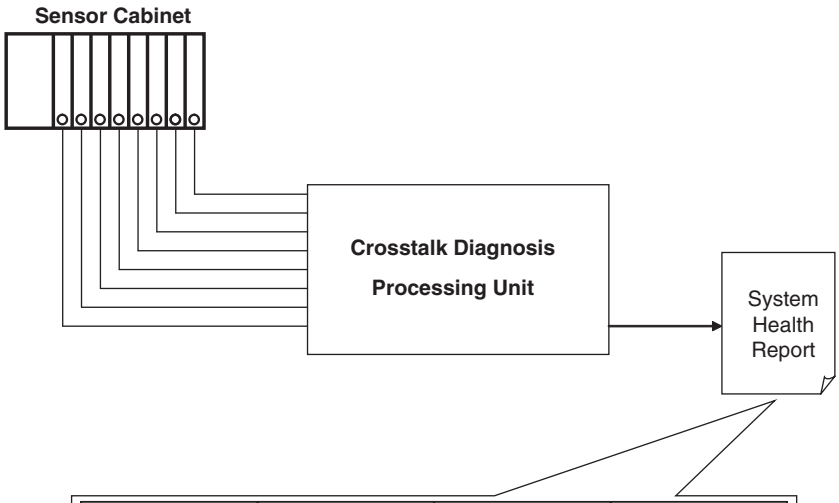

Sensor Channel	Duration of waveform (seconds)	Duration of crosstalk (seconds)	Percentage of signal containing crosstalk (%)
1	86,400	200	0.23
2	86,400	122	0.14
3	86,400	21	0.02
4	86,400	65,988	76.38
5	86,400	32	0.04
6	86,400	59,963	69.40
7	86,400	65	0.08
8	86,400	66,555	77.03

FIGURE 11 Concept diagram of loop diagnostic system.

TABLE 2 Test Configurations for Crosstalk Analysis Data from Various Detectors

Test ID	Detector Name	Date	Duration of Waveform (h:min)	Loop Type	Weather Conditions	Mean Temperature (°F)
1	NA_L6	03/23/2007	2:35	Inductive	Heavy rain	56
2	NA_L8	03/23/2007	2:35	Inductive	Heavy rain	56
3	NB_L6	03/23/2007	2:34	Inductive	Heavy rain	56
4	NB_L8	03/23/2007	2:34	Inductive	Heavy rain	56
5	NA_M1	05/15/2009	0:57	Microloop	Mostly clear	62
6	NA_M7	05/15/2009	0:57	Microloop	Mostly clear	62
7	NB_M7	05/15/2009	0:57	Microloop	Mostly clear	62

how the probabilistic threshold estimated in Figure 4 can be applied to produce a binary characterization of the presence or absence of crosstalk. The application of this binary indicator function to the 14 h of crosstalk indices is summarized in Figure 10 and tabulated in Table 1.

The paper recommends the development of a diagnostic device that can plug into existing loop detector cards, collect data over an extended period (several days), and produce tabular reports, similar to that shown in Table 1, which indicate the proportion of time that a loop detector channel experiences crosstalk. The authors envision that such a device would drill down the reporting capability to examine data archives in a format similar to that shown in Figure 9 for a user-defined time window.

ACKNOWLEDGMENTS

This work was supported by NCHRP and Purdue University.

REFERENCES

1. Switzer, R. B. Inductive Loop Vehicle Detector. U.S. Patent 3,492,637. 1970.
2. *Traffic Detector Handbook,* Vol. II, 3rd ed. FHWA-HRT-06-139. FHWA, U.S. Department of Transportation, Oct. 2006.
3. Bhagat, V., and D. L. Woods. Loop Detector Crosstalk. *ITE Journal,* Vol. 67, No. 2, Feb. 1997, pp. 36–49.
4. Haoui, A., R. Kavaler, and P. Varaiya. Wireless Magnetic Sensors for Traffic Surveillance. *Transportation Research Part C,* Vol. 16, 2008, pp. 294–306.
5. Mills, M. K. Inductive Loop Detector Analysis. *Proc., Vehicular Technology Conference, 1981, 31st IEEE,* Vol. 31.
6. Coifman, B. Using Dual Loop Speed Traps to Identify Detector Errors. In *Transportation Research Record: Journal of the Transportation Research Board, No. 1683,* TRB, National Research Council, Washington, D.C., 1999, pp. 47–58.
7. Park, U., F. Silva, M. Hou, J. Heidemann, G. Guiliano, X. Wang, and N. Prashar. *Single- and Multi-Sensor Techniques to Improve Accuracy of Urban Vehicle Classification.* ISI-TR-2006-614, USC Information Sciences Institute, University of Southern California, Los Angeles, 2006.
8. Jefferis, B. C. Inductive Loop Presence Detector with Cross Talk Filter. U.S. Patent 4,873,494. 1986.
9. Kay, S. M. *Fundamentals of Statistical Signal Processing: Volume II, Detection Theory.* Prentice Hall, Upper Saddle River, N.J., 1993, pp. 60–71.

The contents of this paper reflect the views of the authors, who are responsible for the facts and accuracy of the data, and do not necessarily reflect the official views or policies of NCHRP. These contents do not constitute a standard, specification, or regulation.

The Traffic Signal Systems Committee peer-reviewed this paper.